Journal of Applied Geophysics 68 (2009) 219–230

Contents lists available at ScienceDirect

Journal of Applied Geophysics

journal homepage: www.elsevier.com/locate/jappgeo

Site classification and estimation of surface level seismic hazard using geophysical data and probabilistic approach

P. Anbazhagan *, T.G. Sitharam, K.S. Vipin

Civil Engineering Department, Indian Institute of Science, Bangalore-12, India

ARTICLE INFO

Article history:
Received 5 July 2008
Accepted 12 November 2008

Keywords:
MASW
Site class
Probabilistic
Seismic hazard
Response spectrum

ABSTRACT

This paper presents the site classification of Bangalore Mahanagar Palike (BMP) area using geophysical data and the evaluation of spectral acceleration at ground level using probabilistic approach. Site classification has been carried out using experimental data from the shallow geophysical method of Multichannel Analysis of Surface wave (MASW). One-dimensional (1-D) MASW survey has been carried out at 58 locations and respective velocity profiles are obtained. The average shear wave velocity for 30 m depth (Vs^{30}) has been calculated and is used for the site classification of the BMP area as per NEHRP (National Earthquake Hazards Reduction Program). Based on the Vs^{30} values major part of the BMP area can be classified as "site class D", and "site class C". A smaller portion of the study area, in and around Lalbagh Park, is classified as "site class B". Further, probabilistic seismic hazard analysis has been carried out to map the seismic hazard in terms spectral acceleration (S_a) at rock and the ground level considering the site classes and six seismogenic sources identified. The mean annual rate of exceedance and cumulative probability hazard curve for S_a have been generated. The quantified hazard values in terms of spectral acceleration for short period and long period are mapped for rock, site class C and D with 10% probability of exceedance in 50 years on a grid size of 0.5 km. In addition to this, the Uniform Hazard Response Spectrum (UHRS) at surface level has been developed for the 5% damping and 10% probability of exceedance in 50 years for rock, site class C and D. These spectral acceleration and uniform hazard spectrums can be used to assess the design force for important structures and also to develop the design spectrum.

1. Introduction

The microzonation and site response studies require the characterization of subsurface soil properties of the site. The general site characterization comprises of the evaluation of subsurface features, material types, material properties and buried/hollow structures, by which it is determined whether the site is safe against earthquake effects like site response, lateral spread and liquefaction. A number of geophysical methods have been proposed for near-surface characterization and measurement of shear wave velocity using a large variety of testing configurations, processing techniques, and inversion algorithms. The most widely used techniques for seismic site characterizations are SASW (Spectral Analysis of Surface Waves) and MASW (Multichannel Analysis of Surface Waves). The spectral analysis of surface wave (SASW) method has been used for site investigation for several decades by Nazarian et al. (1983), Al-Hunaidi (1992), Stokoe et al. (1994), Tokimatsu (1995), and Ganji et al. (1997). In SASW method, the spectral analysis of a surface wave is generated by an impulsive source and recorded by a pair of receivers. Evaluating and distinguishing signal from noise using a pair of receivers, as followed in this method is difficult. Thus to eliminate inherent difficulties, a new technique incorporating multichannel analysis of surface waves using active sources, MASW, was developed (Park et al., 1999; Xia et al., 1999; Xu et al., 2006). The MASW has been found to be a more efficient in unraveling the shallow subsurface properties (Park et al., 1999; Xia et al., 1999; Zhang et al., 2004). MASW is increasingly being used in earthquake geotechnical engineering for microzonation and site response studies. MASW is non-intrusive and less time consuming geophysical method.

The widely used approach to estimate seismic-design loads for engineering projects is probabilistic seismic-hazard analysis (PSHA). The primary output from a PSHA is a hazard curve showing the variation of a selected ground-motion parameter, such as peak ground acceleration (PGA) or spectral acceleration (S_a), against the annual frequency of exceedance (or its reciprocal, return period). The design value is the ground-motion level that corresponds to a preselected design return period (Bommer and Abrahamson, 2006). PSHA is able to reflect the actual hazard level due to earthquakes along with bigger and smaller events, which are also important in hazard estimation, due to their higher occurrence rates (Das et al., 2006).

In this study, an attempt has been made to classify the BMP area using 30 m average shear wave velocity obtained from MASW survey. MASW field test have been carried out at 58 locations and one dimensional shear wave velocity is measured. These values are used to

* Corresponding author.
E-mail address: anbazhagan@civil.iisc.erent.in (P. Anbazhagan).

0926-9851/$ – see front matter © 2008 Published by Elsevier B.V.
doi:10.1016/j.jappgeo.2008.11.001

estimate equivalent shear wave velocity and are used to classify the area as per NEHRP. Further, the PSHA has been carried out to estimate the seismic hazard parameters and response spectrum at ground level considering the site classes and six seismogenic sources given by Anbazhagan et al. (2008). The study area is divided into grids of size of 0.5 km × 0.5 km, hazard parameters are estimated at the center of each grid cell using a newly developed MATLAB program. The quantified hazard in terms of the ground level spectral acceleration values for short period of 0.01 s and long period of 1 s are mapped with 10% probability of exceedance in 50 years for site class C and D, which corresponds to a return periods of nearly 475 years. In addition to this, the Uniform Hazard Response Spectra (UHRS) has also been developed.

2. Study area and testing programme

The Bangalore city covers an area of approximately 696.17 km^2 (Greater Bangalore). The area of study is limited to Bangalore Metropolis area (Bangalore Mahanagar Palike, BMP) of about 220 km^2. Bangalore is situated at a latitude of 12° 58′ North and longitude of 77° 36′ East and is at an average altitude of around 910 m above mean sea level (MSL). It is the principal administrative, industrial, commercial, educational and cultural capital of Karnataka state and lies in the South-Western part of India (see Fig. 1). Bangalore is one of the fastest growing cities and it is the fifth biggest city in India. Besides political activities, Bangalore houses many national research and development laboratories, defense establishments, small and large-scale industries and it is the major hub of information technology firms. The rapid growth of population density has resulted in mushrooming of all types of buildings and most of these new buildings are coming up in filled up areas. This along with improper construction practices makes Bangalore is vulnerable even against moderate earthquakes (Sitharam et al., 2006). As per BIS 1893 (2002) Bangalore has been upgraded to Zone II from Zone I in the seismic zonation map. Recent studies by Ganesha Raj and Nijagunappa (2004), Sitharam et al. (2006), Sitharam and Anbazhagan (2007) suggested that Bangalore need to be upgraded from seismic zone II to zone III based on the regional seismotectonic details and hazard analysis.

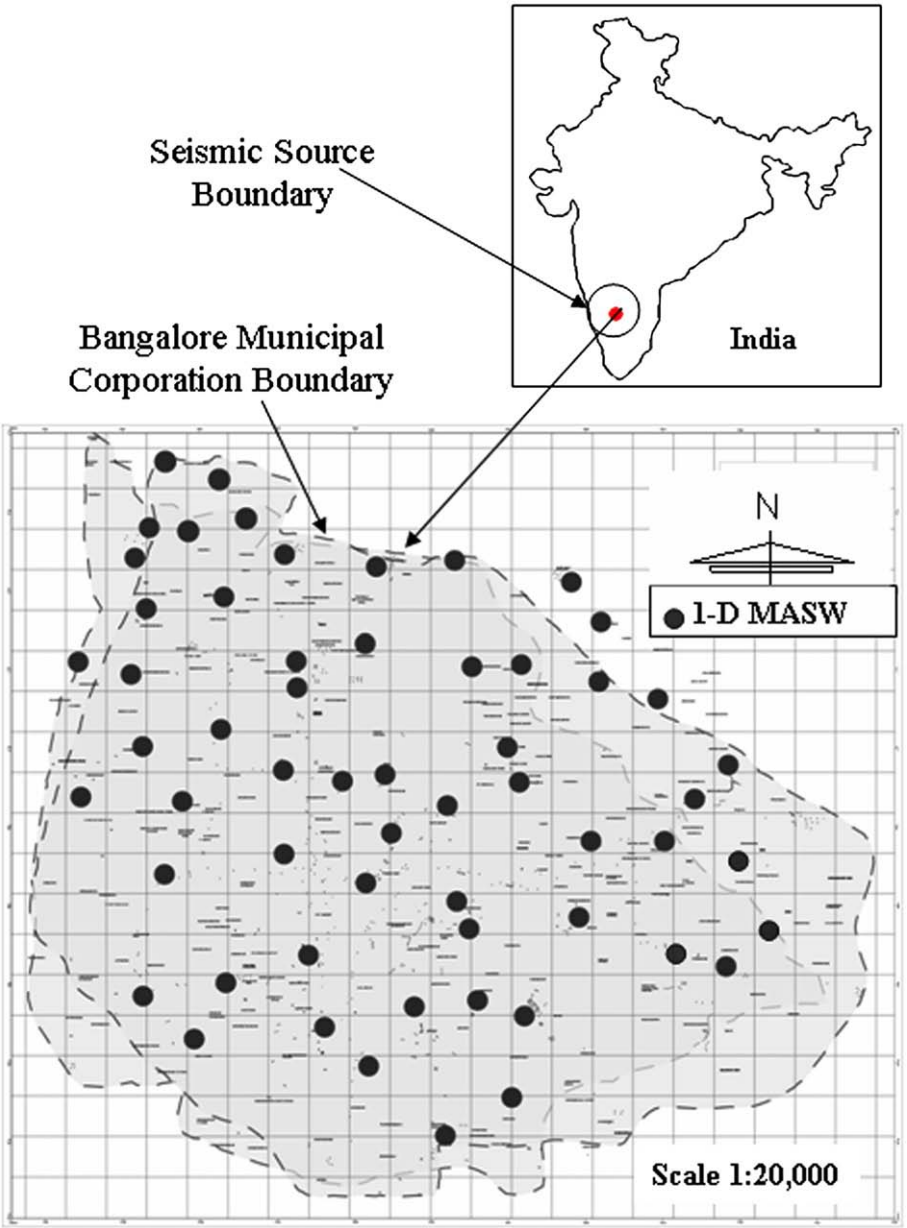

Fig. 1. Study area along with in India map and MASW testing locations.

In this study geophysical test of MASW has been carried out at 58 selected locations and it is shown in Fig. 1 along with the map of India. The test locations are selected such a way that they represent the entire city subsurface information. 58 one-dimensional (1-D) surveys have been carried out at flat ground and also in important places like parks, hospitals, schools and temple yards, etc. MASW is a geophysical method, which generates a shear-wave velocity (*Vs*) profile (i.e., *Vs* versus depth) by analyzing Raleigh-type surface waves on a multi-channel record. MASW system consisting of 24 channels Geode seismograph with 24 vertical geophones of 4.5 Hz capacity, impulsive source of 6.8 kg (sledge hammer) with 300mmx300 mm size hammer plate and connecting cables with computing field laptop.

3. Data collection and acquisition

Geophones are rigidly fixed in the field in straight line with required intervals and interconnected with cables and these are then connected to Geode seismograph. Impulsive source of sledge hammer is connected through hammer cable to geode with necessary battery for power. The seismic waves are created by impulsive source of 6.8 kg (sledge hammer) with 300 mm × 300 mm size hammer plate. These waves are captured by vertical geophones/receivers at sample interval of 0.125 ms to a sample length of 1 s and further analyzed using SurfSeis software. The optimum field parameters such as source to first and last receiver, receiver spacing and spread length of survey lines are selected in such a way that required depth of information can be obtained. These are in conformity with the recommendations of Park et al. (2002) and Xu et al. (2006). All tests have been carried out with geophone interval of 1 m. Source has been kept on both side of the spread and source to the first and last receiver were also varied from 5 m, 10 m and 15 m to avoid the effects of near-field and far-field. The seismic waves are created by impulsive source hammer plate through multiple (up to 10) shots. These waves are captured by geophones/receivers and the captured Rayleigh wave is further analyzed using SurfSeis software. SurfSeis is designed to generate *Vs* data (either in 1-D or 2-D format) using a simple three-step procedure: i) preparation of a Multichannel record (some times called a shot gather or a field file), ii) dispersion-curve analysis, and iii) inversion. Typical recorded surface wave arrivals using source to first receiver distance as 5 m with recording length of 1000 ms is shown in Fig. 2. Even though MASW usually recorded the strongest energy, complications often arise due to inclusion of noise. Noise may be random ambient noise (e.g., traffic and machinery noise), source-generated body waves (e.g., direct, refracted, scattered, and reflected compressional waves), and higher-mode surface waves. Effectiveness of a particular surface-wave method depends on exclusion of noise during data acquisition and processing stages. In most of data, noise has been controlled by using critical acquisition parameters and recording time. At few locations, data was contaminated with noise, those data noise has been removed during the processing. Typical recorded data with noise is presented in Fig. 2 (a) and after removing noise is presented in 2(b).

The generation of a dispersion curve is an important step in shear wave velocity profiling which represents the nature of subsurface material. A dispersion curve is generally displayed as a function of phase velocity versus frequency. Phase velocity can be calculated from the linear slope of each component on the swept-frequency record. In this study the lowest analyzable frequency is around 4 Hz and highest frequency of 75 Hz has been considered to produce dispersion curve. Typical dispersion curve is shown in Fig. 3. In all the data noise are eliminated and dispersion curves are developed corresponding to high signal to noise ratio of 80 and above.

Dispersion curves obtained are further used to develop a 1-D shear wave velocity profiles. Shear wave velocity profile has been obtained using an iterative inversion process that requires the dispersion curve developed earlier as input. A least-squares approach allows automation

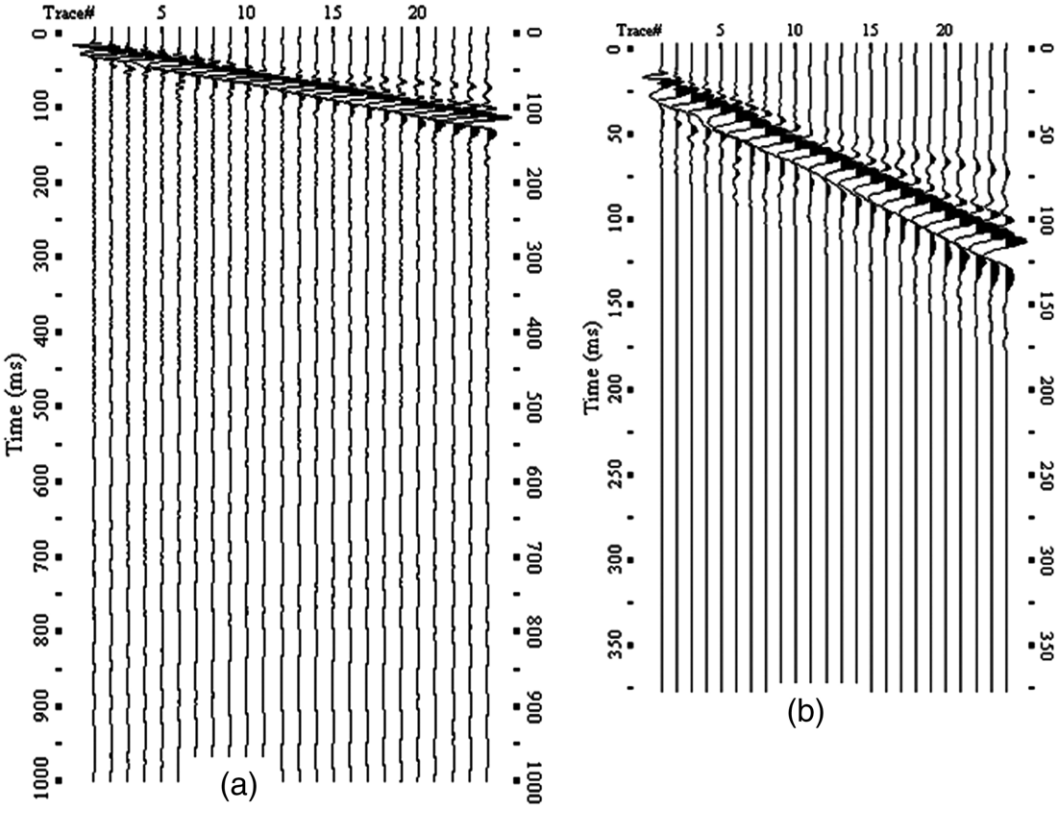

Fig. 2. Typical Recorded data in the filed (a) contaminated with noise and (b) Processed data after removing noise.

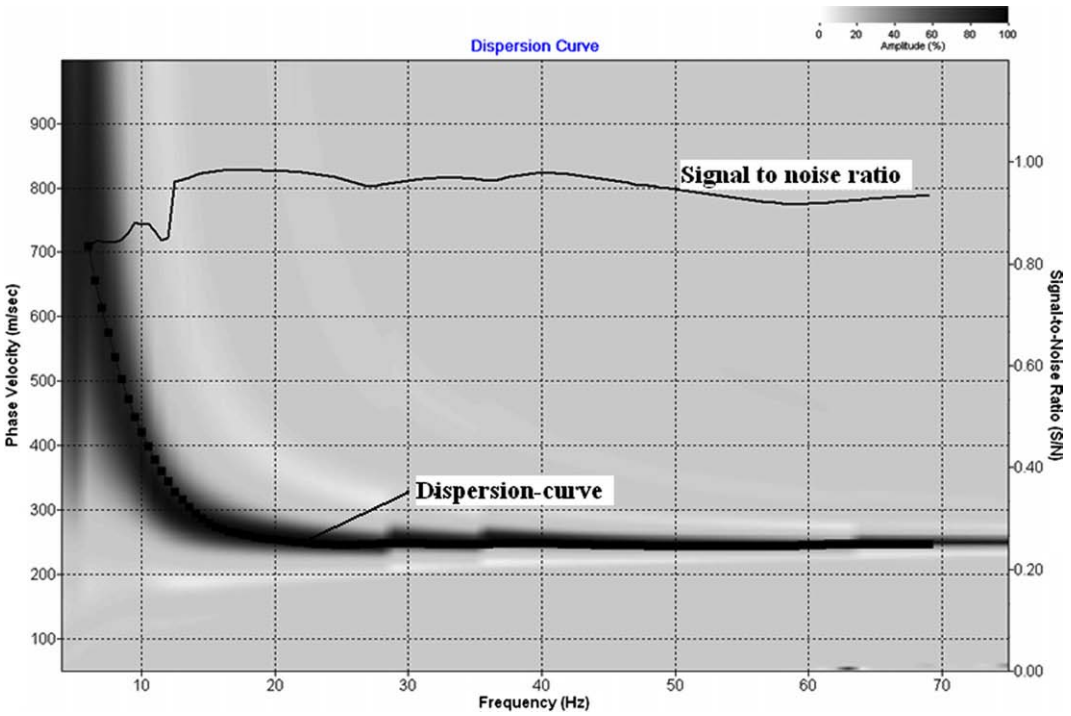

Fig. 3. Typical dispersion curve after removing noise.

of the process (Xia et al., 1999) which is inbuilt in SurfSeis. Shear wave velocity has been updated after completion of each iteration with other parameters such as Poisson's ratio, density, and thickness of the model remaining unchanged. An initial earth model is specified to begin the iterative inversion process. The earth model consists of velocity (P-wave and S-wave velocity), density, and thickness parameters. Typical one-dimensional shear wave velocity profile is shown in Fig. 4.

4. Site classification

To ascertain the effect of earthquake shaking on the ground surface, site characterization by evaluating shear wave velocity at shallow depth would be essential. The seismic site characterization for calculating seismic hazard is usually carried out based on the near-surface (30 m) shear wave velocity values. Equivalent velocity for top 30 m (Vs^{30}) depth

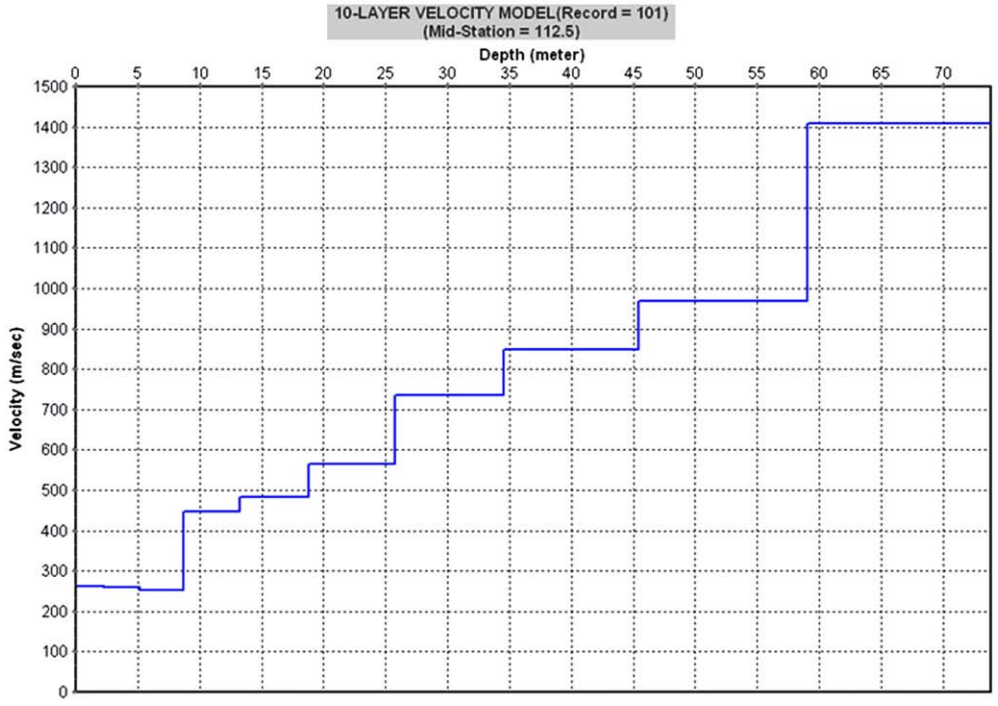

Fig. 4. Typical one-dimensional shear wave velocity profile.

is used for site classification in the NEHRP recommendation and also International building code (IBC) classification (International Building Code, 2000) (Dobry et al., 2000; Kanli et al., 2006). To classify the study area, the shear wave velocity ranges suggested by NEHRP (The Building Seismic Safety Council (BSSC, 2001), are site class A (Vs^{30}>1.5 km/s), site class B (0.76 km/s<Vs^{30}≤1.5 km/s), site class C (0.36 km/s<Vs^{30}≤ 0.76 km/s) and site class D (0.18 km/s<Vs^{30}≤0.36 km/s) have been considered. The equivalent shear wave velocity up to a depth of 30 m (Vs^{30}) is computed in accordance as follows:

For 30 m average depth, shear wave velocity is written as;

$$Vs^{30} = \frac{30}{\sum_{i=1}^{N}\left(\frac{d_i}{v_v}\right)} \quad (1)$$

where d_i and v_i denote the thickness (in meters) and shear-wave velocity (at a shear strain level of 10^{-5} or less, m/s) of the ith formation or layer respectively, in a total of N layers, existing in the top 30 m. A spread sheet has been used to carry out the calculation in 58 locations. The site classes based on 30 m equivalent shear wave velocity is considered for site amplification and site response studies. A typical 30 m equivalent shear wave velocity (Vs^{30}) for the study area is shown in Fig. 5. The Vs^{30} shows that study area can be classified "site class D, C and B" as per NEHRP recommendations. However major part of study area is falls in site C and D, only these two classes considered for estimation ground level hazard values.

5. Seismicity and seismic sources

Many researchers have addressed the intra plate earthquakes and seismicity of south India (Purnachandra Rao, 1999; Ramalingeswara Rao, 2000; Iyengar and RaghuKanth, 2004). Many devastating earthquakes in recent times (Koyna, 1967; Killari, 1993, Jabalpur, 1997; Bhuj, 2001) have occurred in south India, a region that was previously considered as stable and aseismic shield region. This region has also experienced many earthquakes of magnitude of 6.0 since the 18th Century and some of which were disastrous (Ramalingeswara Rao, 2000). Among them are the Mahabaleshwar (1764), Kutch (1819), Damooh hill (Near Jabalpur, 1846), Mount Abu (1848), Coimbatore (1900), Son-Valley (1927), Satpura (1938), Koyna, (1967), Latur (1993), and Jabalpur earthquake (1997). Nath (2006) highlighted that the most common cause for higher seismicity of the Indian shield appears to be

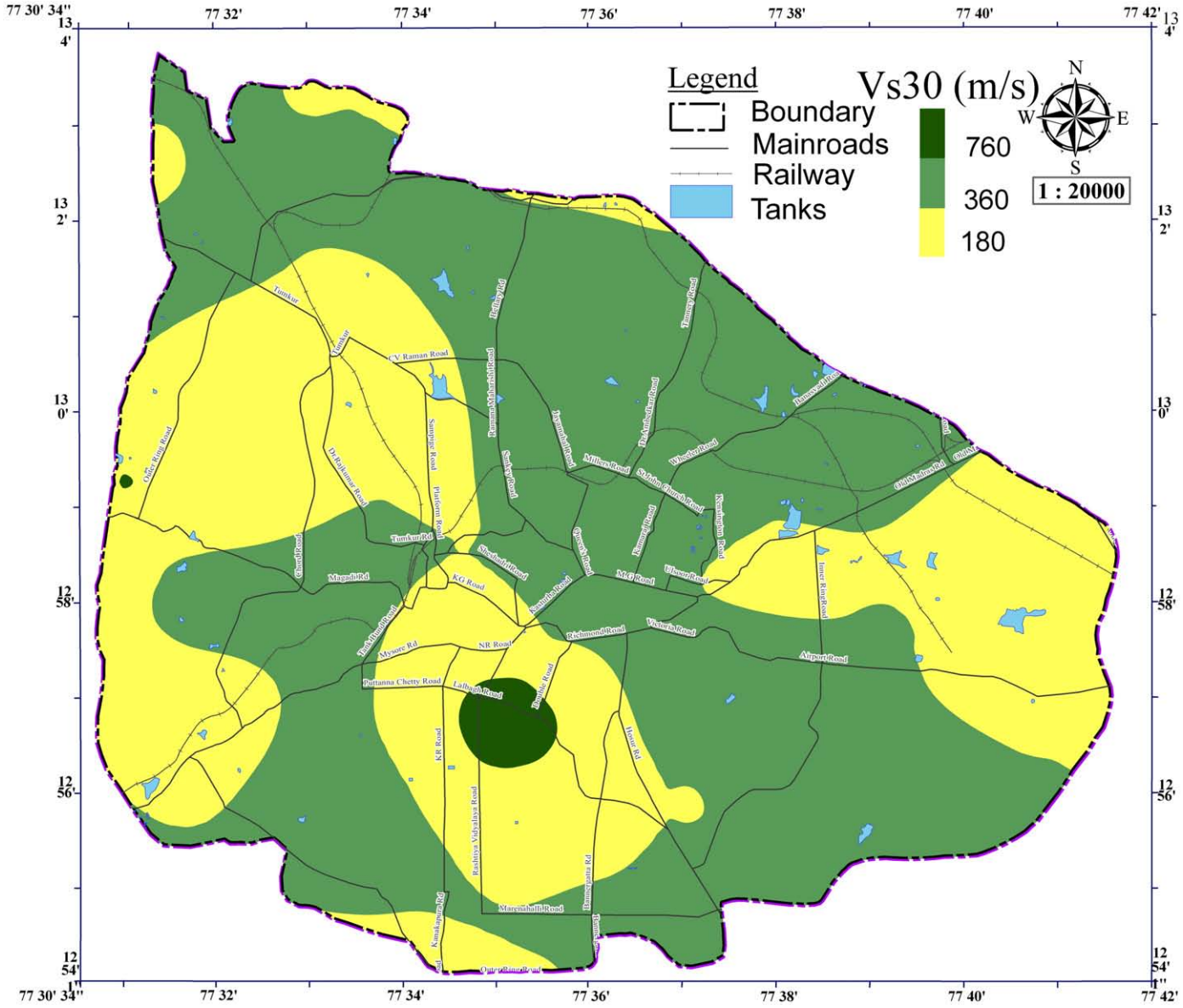

Fig. 5. Equivalent shear wave velocity for 30 m depth.

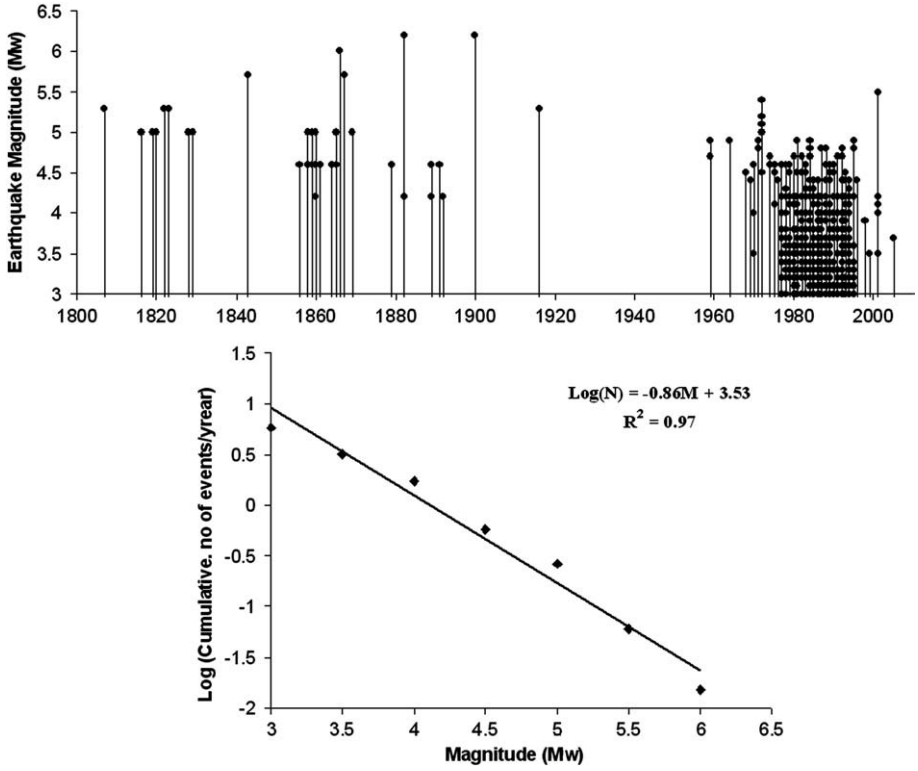

Fig. 6. The time history of historic and instrumented (total) data with corresponding frequency magnitude distribution plot.

due to the compressive stress field in the Indian shield oriented in NNE-SSW direction due to the India-Eurasia plate collision. Sridevi Jade (2004) highlighted that southern peninsular India moves as a rigid plate with about 20 mm/year velocity in the NNE direction (using Global positioning system measurement at Indian Institute of Science, Bangalore). Sitharam et al. (2006) and Sitharam and Anbazhagan (2007) have presented the DSHA and have identified the seismogenic sources and maximum credible earthquake (MCE) for Bangalore in south India. Authors have carried out extensive study and prepared a new seismotectonic atlas of 350 km radius around Bangalore. Authors have carried out detailed hazard analysis to identify the seismogenic sources, which are presented in Sitharam et al. (2006) and Sitharam and Anbazhagan (2007). They highlighted that PGA evaluated of Bangalore is much more than values recommended in India seismic code (BIS 1893, 2002). Anbazhagan et. al., (2008) estimated the seismic parameter of 'b' using (1) Gutenberg and Richter recurrence law (Gutenberg and Richter, 1944) and (2) Kijko and Sellevoll (1989, 1992) maximum likely hood method utilizing extreme, instrumented and complete catalogs. The authors have reported that 'b" value of region has increased when compared to past. Fig. 6 presents the time history of historic and instrumented (total) data with corresponding frequency magnitude distribution plot, which as follows:

$$log(N) = 3.52 - 0.86M. \quad (2)$$

This recurrence relation includes all the data of micro- major earthquakes in the region and has high a correlation coefficient of 0.97 (Anbazhagan et al., 2008).

Seismic sources having PGA of more than 0.035 g (from deterministic hazard analysis) and located within 150 km radius from Bangalore are considered as vulnerable seismic sources for probabilistic approach. The details of 6 sources with reported number of earthquake data close to each source are given in Table 1. The shortest and longest distance from the Bangalore city to these sources are presented in Table 1. These distances are used to calculate the hypocentral distances by assuming a focal depth of 15 km for all the sources (Sitharam and Anbazhagan, 2007). These sources have been used here to map the peak ground acceleration by considering local site classification to account site effects. The seismogenic sources considered in this study is shown in Fig. 7. In Fig. 7, F47 and F19 are faults and L15, L16, L20 and L22 are the active lineaments.

6. Probabilistic approach

PSHA is the most widely used approach to evaluate the seismic design load for important engineering projects. PSHA method was initially developed by Cornell (1968) and its computer program was developed by McGuire (1976, 1978) and Algermissen and Perkins (1976). In PSHA, the ground motion parameters are estimated for the selected values of probability of ground motion exceedance during the design period of the structures or for selected values of annual frequency or return period for ground motion exceedance. The occurrence of an earthquake in a seismic source is assumed to follow a Poisson's distribution. The probability of ground motion parameter at a given site, Z, will exceed a specified level, z, during a specified time, T and it is represented by the expression:

$$P(Z > z) = 1 - e^{-\nu(z)T} \leq \nu(z)T \quad (3)$$

where $\nu(z)$ is the mean annual rate of exceedance of ground motion parameter, Z, with respect to z. The function $\nu(z)$ incorporates the uncertainty

Table 1
Seismic source parameters.

Number and name of source		Hypocentral distance (km)		Length (km)	No EQ close to source
		Min	Max		
F19	Mettur East Fault	98	117	38	15
F47	Arkavati Fault	53	89	125	20
L15	Mandya–Channapatna–Bangalore	16	105	105	25
L16	Arakavathi–Doddaballapur	24	78	109	12
L20	Chelur–Kolar–Battipalle	60	105	111	50
L22	Nelamangala–Shravanabelagula	30	151	130	14

Fig. 7. Seismogenic sources considered for the PSHA.

in time, size and location of future earthquakes and uncertainty in the level of ground motion they produce at the site. It is given by:

$$v(z) = \sum_{n=1}^{N} N_n(m_0) \int_{m=m^0}^{m^u} f_n(m) \left[\int_{r=0}^{\infty} f_n(r|m) P(Z > z|m,r) dr \right] dm \quad (4)$$

where N_n (m_0) is the frequency of earthquakes on a seismic source n, having a magnitude higher than a minimum magnitude m^0 (in this study it is taken as 4.0). $f_n(m)$ is the probability density function for a minimum magnitude of m^0 and a maximum magnitude of m^u; $f_n(r|m)$ is the conditional probability density function (probability of occurrence of an earthquake of magnitude m at a distance r from the site for a seismic source n); $P(Z>z|m, r)$ is the probability at which the ground motion parameter Z exceeds a predefined value of z, when an earthquake of magnitude m occurs at a distance of r from the site. The integral in Eq. (4) can be replaced by summation and the density functions $f_n(m)$ and $f_n(r|m)$ can be replaced by discrete mass functions. The resulting expression for $v(z)$ is given by:

$$v(z) = \sum_{n=1}^{N} \sum_{m_i=m^0}^{m_i=m^u} \lambda_n(m_i) \left[\sum_{r_j=r_{min}}^{r_j=r_{max}} P_n\left(R = r_j|m_i\right) P\left(Z > z|m_i, r_j\right) \right] \quad (5)$$

where λ_n (m_i) is the frequency of occurrence of magnitude m_i at the source n obtained by discretizing the earthquake recurrence relationship for the source n.

The magnitude recurrence model for a seismic source specifies the frequency of seismic events of various sizes per year. The seismic parameters are determined using Gutenberg–Richter (G–R) magnitude-frequency relationship which is given in Eq. (2). The maximum magnitude (m^u) is taken as 6 for each source based on maximum likely hood method presented by Anbazhagan et al., (2008). The recurrence relation for each fault, capable of producing earthquake magnitudes in the range m^0 to m^u is calculated using the truncated exponential re-currence model developed by McGuire and Arabasz (1990).

The recurrence relation Eq. (2) developed for the study area represents the entire region and it is not for specific source. Evaluation of separate source recurrence rate is necessary to discriminate nearby sources from far-off sources and to differentiate the activity rate among sources. Such seismic source recurrence relation is rarely known due to paucity of large-scale data accruing in historical times. An alternative is to empirically calculate the "b" value from known measured slip rate of each seismic source. For the sources under consideration, no such slip rate measurements are reported. Moreover, PI earthquakes are associated with poor surface expressions of faults and hence reliable estimation of slip rates are not available (Anbazhagan et al., 2008). Hence, it is necessary to proceed on a heuristic basis invoking the principle of conservation of seismic activity. Deaggregation procedure followed here is similar to the one followed by Iyengar and Ghosh (2004), RaghuKanth and Iyengar (2006) and Anbazhagan et al. (2008) for PSHA of Delhi, Mumbai and Bangalore respectively.

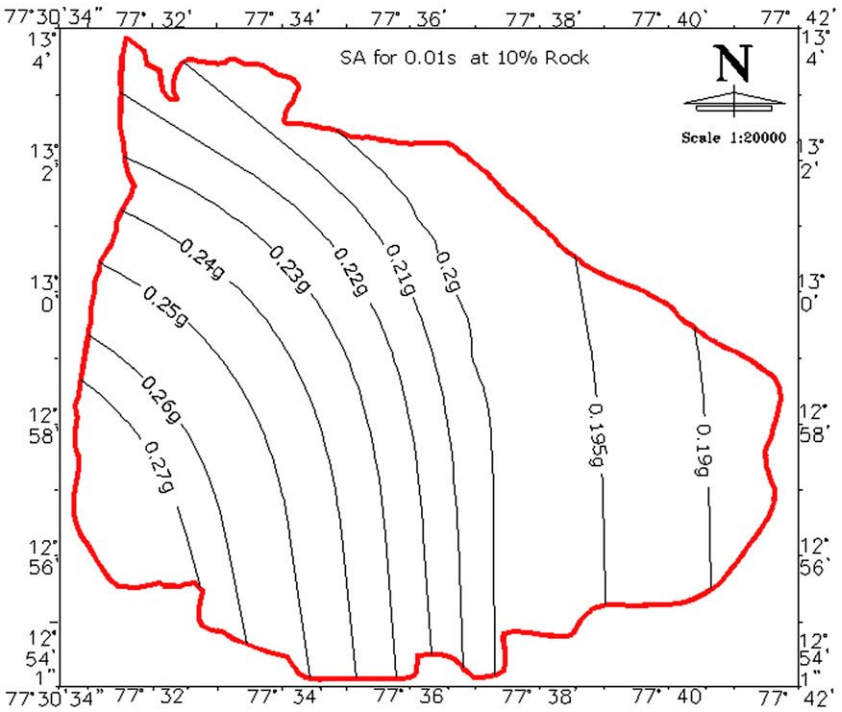

Fig. 8. Spectral acceleration for 0.01 s at rock level.

In PSHA, the probability of occurrence of an earthquake anywhere in the fault is assumed to be same. The uncertainty involved in the source to site distance is described by a probability density function. The shortest and longest distance from each source to the centre of the grid is calculated (distances from Vidhana Soudha to all the sources are presented in Table 1). The conditional probability distribution function of the hypocentral distance R for an earthquake of magnitude $M = m$ is assumed to be uniformly distributed along a fault. It is given by Kiureghian and Ang (1977).A cumulative distance probability for each source has been estimated.

Since the study area is located in peninsular India, the attenuation relation (for peak horizontal acceleration and spectral acceleration) for the rock site in Peninsular India developed by RaghuKanth and Iyengar (2007) has been used. The attenuation relation suggested for the region is:

$$lny = c_1 + c_2(M - 6) + c_3(M-6)^2 - lnR - c_4R + ln(\in) \quad (6)$$

where y, M, R and ε refer to PGA/spectral acceleration (g) at the bed rock level, moment magnitude, hypocentral distance and error associated with the regression respectively. The coefficients in Eq. (6), c_1,

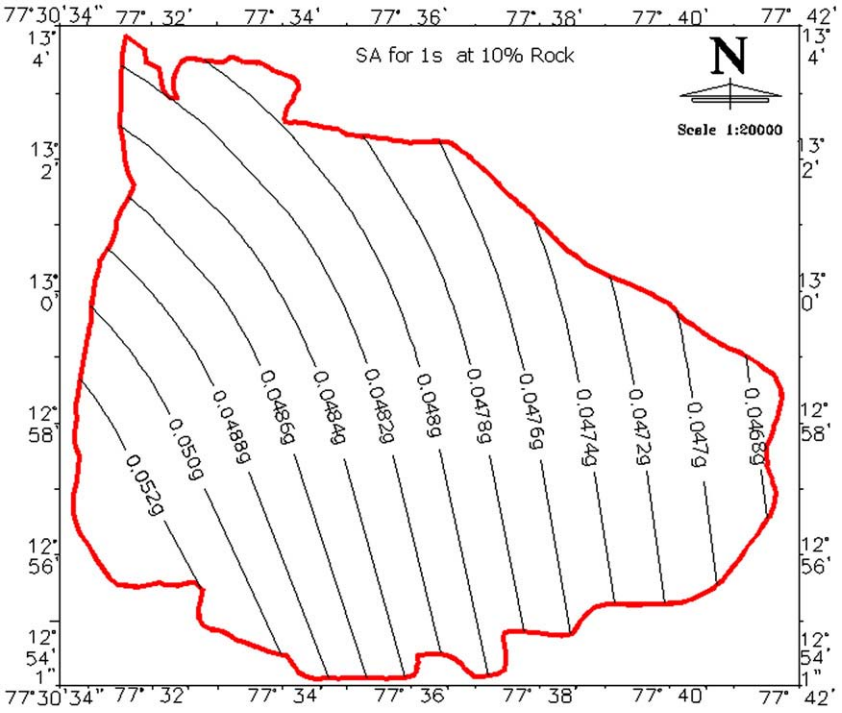

Fig. 9. Spectral acceleration for 1.0 s at rock level.

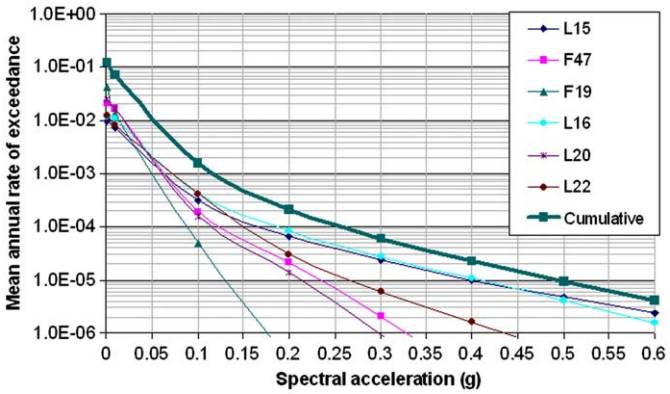

Fig. 10. Spectral acceleration at surface level corresponding to period of 1 s and 5% damping for Bangalore.

c_2, c_3, and c_4 are obtained from RaghuKanth and Iyengar (2007). The normal cumulative distribution function has a value which is most efficiently expressed in terms of the standard normal variables (z) which can be computed for any random variables using transformation as given below (Kramer, 1996):

$$z = \frac{lnPGA - \overline{lnPGA}}{\sigma_{lnPGA}} \tag{7}$$

where PGA is the various targeted peak acceleration levels which will be exceeded. $\overline{lnPGA}$ is the value calculated using attenuation relationship equation and $\sigma_{\ln PGA}$ is the uncertainty in the attenuation relation expressed by the standard deviation.

7. Evaluation of seismic hazard considering site effects

Based on site classes (soil type, thickness and strength) the surface level peak ground acceleration (PGA) and spectral acceleration values can be different from the rock level values. For estimating the surface level spectral acceleration values, a new empirical attenuation relation has been proposed for generating design response spectra for engineering structures the by RaghuKanth and Iyengar (2007) for Peninsular India were used.

$$lnF_s = a_1 y_{br} + a_2 + ln\delta_s \tag{8}$$

where a_1 and a_2 are regression coefficients, y_{br} is the spectral acceleration at rock level and δ_s is the error term. The value of spectral acceleration for different site classes can be obtained using Eq. (9).

$$y_s = y_{br} F_s \tag{9}$$

where y_s is the spectral acceleration at the ground surface for a given site class.

For generating seismic hazard curves, a newly developed MATLAB program was used. The input for this program include the details of the faults, viz. latitude and longitude of the starting and end point of the faults, number of earthquakes along the fault and the maximum magnitude and the seismicity parameters. The program will divide the study area into small grids of size of 0.5 km × 0.5 km, the grid size can also be specified as an input parameter, and the seismic hazard values at the centre of each of the grid will be calculated. The hazard curves of mean annual rate of exceedance versus PGA and spectral acceleration for 0 to 4 s at rock as well as ground level were calculated for each of the grid cells. Peak ground acceleration at rock level for 10% probability of exceedance in 50 years is presented in Anbazhagan et al. (2008).

The frequency content of an earthquake motion will strongly influence the effects of ground motion and hence the PGA value on its own cannot characterize the ground motion. A response spectrum is used extensively in earthquake engineering practice to indicate the frequency content of an earthquake motion. A Response Spectrum describes the maximum response of a single-degree-of-freedom (SDOF) system to a particular input motion as a function of the natural frequency/period and damping ratio of the SDOF system. The combined influences of acceleration amplitudes and frequency components of the movement are represented in a single graph. To develop the design spectral response spectrum for the design of building needs spectral

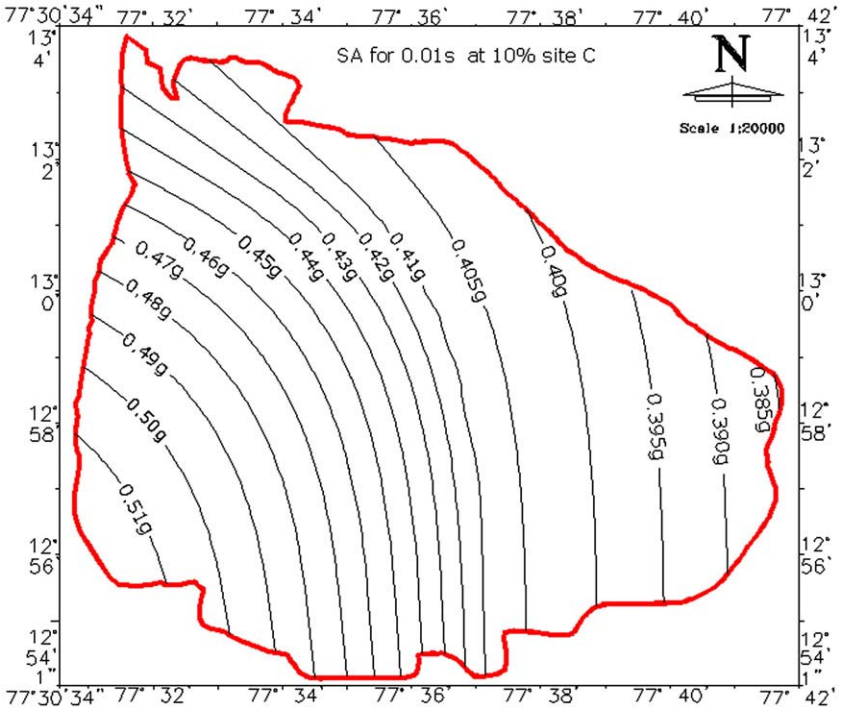

Fig. 11. Spectral acceleration for 0.01 s at surface for site class C.

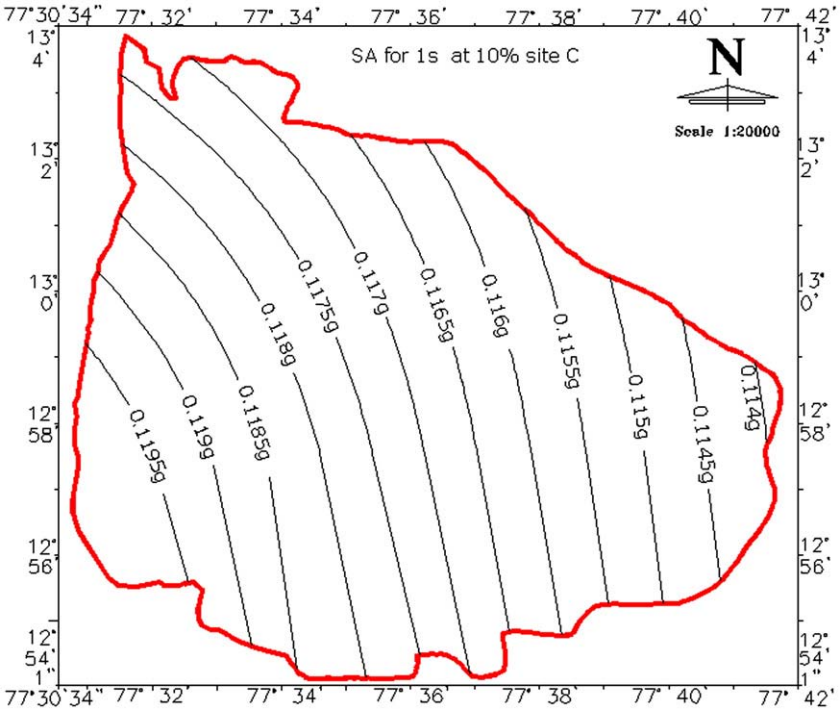

Fig. 12. Spectral acceleration for 1 s at surface for site class C.

acceleration at short periods (0.01 s) and long periods (1 s) (BSSC, 2001). Spectral acceleration distributions for 0.01 s and 1 s at rock level for study area for 10% probability of exceedance in 50 years are shown in Figs. 8 and 9.

Similarly spectral acceleration for site class C and D has been estimated and mapped for study area for 10% probabilities of exceedance in 50 years. Fig. 10 shows the mean annual rate of exceedance versus spectral acceleration for a period of 0 s and 5% damping considering the "Site class D". Figs. 11 and 12 show the spectral acceleration at 0.01 s and 1 s for site class C at ground level for 10% probabilities of exceedance in 50 years. Similarly Figs. 13 and 14 show the spectral acceleration at 0.01 s and 1 s for site class D at ground level for 10% probabilities of exceedance

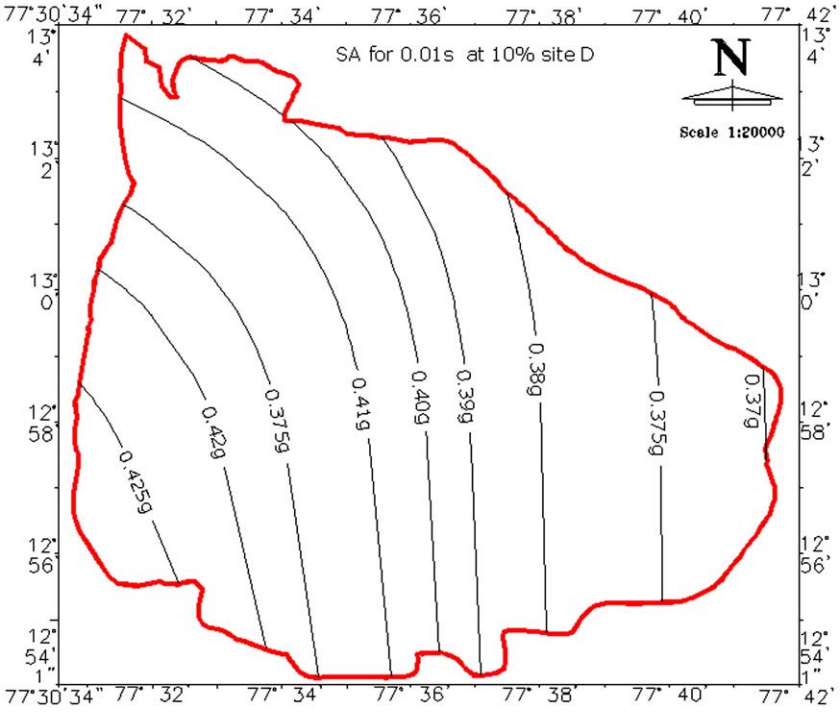

Fig. 13. Spectral acceleration for 0.01 s at surface for site class D.

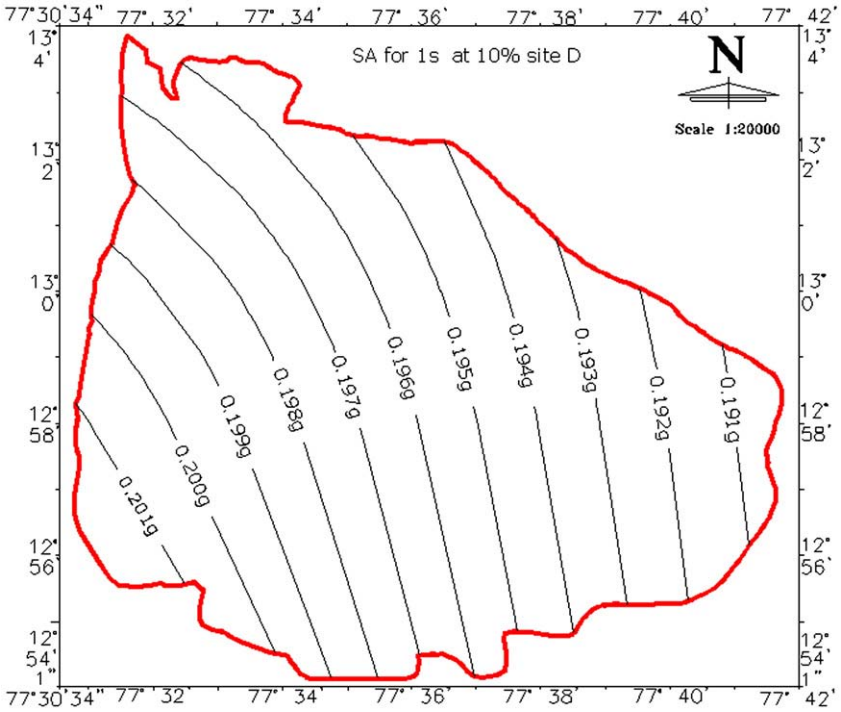

Fig. 14. Spectral acceleration for 1 s at surface for site class D.

in 50 years. Since the time history of the seismic excitation in a certain site is characterized by the corresponding response spectrum, the differences among the time histories of the movements at different places can be analyzed by the comparison of their response spectra. The acceleration-time histories at various depths are obtained as a result of ground response analysis and these motions can be characterized by the corresponding response spectra. Fig. 15 presents the plot of UHRS for 10% probability of exceedance in 50 years rock, site class C and D. A value of PGA (zero peak acceleration, ZPA = PGA) is increased 2.33 times for site class C and 2.5 times for site class D when compared to the rock level PGA value of 0.162 g. The predominant period is 0.04 s for rock, 0.15 s for site class C and 0.18 s for site class D, the results clearly show the variation of predominant frequency with change in soil types. Fig. 15 shows that low period up to 0.15 s spectral acceleration for site class C is larger, after 0.15 s spectral acceleration for site class D is larger.

8. Results and discussions

Most of time the structural engineers are interested in design spectral response acceleration parameters, which are directly used to design structures. The previous section presented spectral acceleration maps for short period and log periods. Figs. 8, 11 and 13 are short

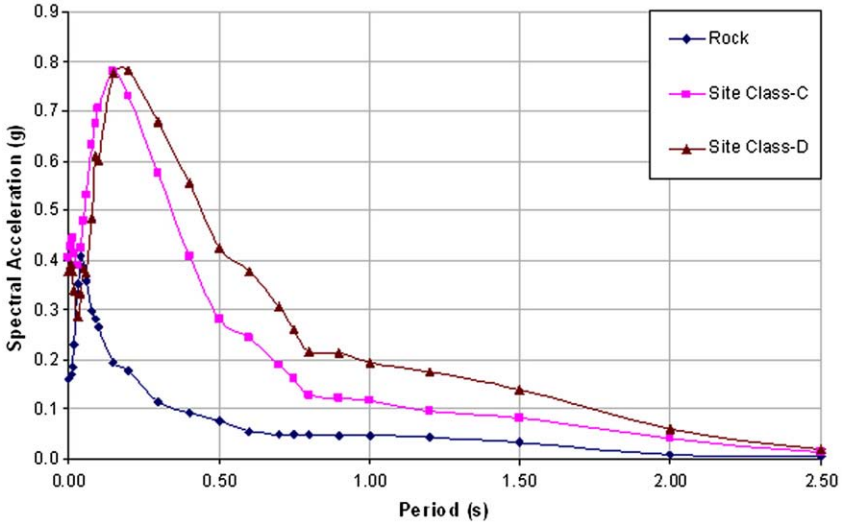

Fig. 15. Typical UHRS with 10% probability of exceedance in 50 years (5% damping) for rock, site class C and D.

period spectral acceleration at rock, site class C and D. These figures show that spectral acceleration values are more at western side of study area decreasing towards the eastern side. This may be attributed to the seismogenic sources location and their orientations. Eastern side has only two sources and the western side has four sources (see Fig. 7). These values are comparable with the PGA map at rock level published by Sitharam et al. (2006). Fig. 8 shows that lowest spectral acceleration value of about 0.19 g observed at eastern side and highest value of about 0.27 g is observed at western side at rock level. Due to the site effect the spectral accelerations are modified, Fig. 11 shows the lowest value is 0.385 g and highest value of about 0.51 g for site class C and the lowest spectral acceleration of 0.37 g and highest of about 0.425 g for site class D as shown in Fig. 13. For the short period site class C shows higher spectral acceleration values when compare to site class D. Figs. 9, 12 and 14 shows the spectral acceleration values for longer periods i.e. 1 s. These figures clearly indicate that for longer periods the spectral acceleration values are much lower than the shorter period values. Figs. 9 and 12 also show that the spectral acceleration does not vary significantly from west to east, but Fig. 14 shows significant variation. Fig. 14 shows the spectral acceleration of about 0.201 g at western side and about 0.191 g at eastern side, these values are much higher when compare to site class C values shown in Fig. 12. For the long period site class D shows higher spectral acceleration values when compare to site class C.

9. Conclusions

Multichannel analysis of surface wave surveys has been carried out at 58 locations in of Bangalore Mahanagar Palike (BMP) area. The equivalent shear wave velocity for the top 30 m depth has been calculated using measured shear wave velocity from MASW. As per NEHRP recommendation the study area can be classified as site class B ($0.76\ km/s < Vs^{30} \leq 1.5\ km/s$), site class C ($0.36\ km/s < Vs^{30} \leq 0.76\ km/s$) and site class D ($0.18\ km/s < Vs^{30} \leq 0.36\ km/s$). However major part of study area comes under site class C and D, which are further considered for spectral acceleration estimation. Surface level spectral acceleration has been estimated for short period and long periods using probabilistic approach for the site class C and D. The study shows that the region has high spectral acceleration values for shorter periods (0.01 s) and lower spectral acceleration for longer periods (1 s). In the short period site class C shows higher spectral acceleration values when compare to site class D. At the same time longer period shows higher spectral acceleration values for site class D when compare to site class C. These mapped spectral acceleration values can be used to develop the design spectrum for structural design.

References

Algermissen, S.T., Perkins, D.M., 1976. A probabilistic estimate of maximum acceleration in rock in the contiguous United States. USGS Open File Report 76-416, p-45.

Al-Hunaidi, M.O., 1992. Difficulties with phase spectrum unwrapping in spectral analysis of surface waves non-destructive testing of pavements. Canadian Geotechnical Journal 29, 506–511.

Anbazhagan, P., Vinod, J.S., Sitharam, T.G., 2008. Probabilistic seismic hazard analysis for Bangalore. Journal of Natural Hazards. doi:10.1007/s11069-008-9253-3 online.

BIS 1893, 2002. Indian Standard Criteria for Earthquake Resistant Design of Structures, Part 1 - General Provisions and Buildings. Bureau of Indian Standards, New Delhi.

Bommer, J.J., Abrahamson, N.A., 2006. Why do modern probabilistic seismic-hazard analyses often lead to increased hazard estimates? BSSA 96 (6), 1967–1977.

BSSC, 2001. NEHRP recommended provisions for seismic regulations for new buildings and other structures 2000 edition, part 1: Provisions, Report no. FEMA 368. Building seismic safety council for the federal emergency management agency, Washington, D.C., USA.

Cornell, C.A., 1968. Engineering seismic risk analysis. BSSA 58, 1583–1606.

Das, S., Guptha, I.D., Guptha, V.K., 2006. A probabilistic seismic hazard analysis of north-east India. Earthquake Spectra 22 (1), 1–27.

Dobry, R., Borcherdt, R.D., Crouse, C.B., Idriss, I.M., Joyner, W.B., Martin, G.R., Power, M.S., Rinne, E.E., Seed, R.B., 2000. New site coefficients and site classification system used in recent building seismic code provisions. Earthquake Spectra 16, 41–67.

Ganesha Raj, K., Nijagunappa, R., 2004. Major lineaments of Karnataka state and their relation to seismicity: remote sensing based analysis. Journal of the Geological Society of India 63, 430–439.

Ganji, V., Gukunski, N., Maher, A., 1997. Detection of underground obstacles by SASW method—numerical aspects. Journal of Geotechnical and Geoenvironmental Engineering 123 (3), 212–219 ASCE.

Gutenberg, B., Richter, C.F., 1944. Frequency of earthquakes in California. BSSA 34, 185–188.

IBC., 2000. International Building Code-2000, 5th Edition. International Code Council: Inc., Falls Church, VA.

Iyengar, R.N., Ghosh, S., 2004. Microzonation of earthquake hazard in greater Delhi area. Current Science 87, 1193–1202.

Iyengar, R.N., RaghuKanth, S.T.G., 2004. Attenuation of strong ground motion in peninsular India. Seismological Research Letters 75 (4), 530–540.

Kanli, A.I., Tildy, P., Pronay, Z., Pinar, A., Hemann, L., 2006. Vs^{30} mapping and soil classification for seismic site effect evaluation in Dinar region. SW Turkey. Geophysical Journal International 165, 223–235.

Kijko, A., Sellevoll, M.A., 1989. Estimation of earthquake hazard parameters from incomplete data files Part I Utilization of Extreme and Complete catalogs with different threshold Magnitudes. BSSA 79, 645–654.

Kijko, A., Sellevoll, M.A., 1992. Estimation of earthquake hazard parameters from incomplete data files. Part II. Incorporating Magnitude Heterogeneity. BSSA 82, 120–134.

Kiureghian, D.A., Ang, A.H.-S., 1977. A fault-rupture model for seismic risk analysis. BSSA 67 (4), 1173–1194.

Kramer, S.L., 1996. Geotechnical Earthquake Engineering. Pearson Education Ptd. Ltd. Reprinted 2003, Delhi, India.

McGuire, R.K., 1976. FORTRAN computer program for seismic risk analysis. U.S. Geol. Surv., Open File Rep. No. 76-67.

McGuire, R.K., 1978. FRISK — A Computer Program for Seismic Risk Analysis. U.S. Department of Interior, Geological Survey: Open-File Report 78-1007.

McGuire, Arabasz, W.J., 1990. In: Ward, S.H. (Ed.), An introduction to probabilistic seismic hazard analysis. Geotechnical and Environmental Geophysics, vol. 1. Society of Exploration Geophysicist, pp. 333–353.

Nath, S.K., 2006. Seismic Hazard and Microzonation Atlas of the Sikkim Himalaya. Department of Science and Technology, Government of India, India.

Nazarian, S., Stokoe II, K.H., Hudson, W.R., 1983. Use of spectral analysis of surface waves method for determination of moduli and thicknesses of pavement systems. Transportation Research Record 930, 38–45.

Park, C.B., Miller, R.D., Miura, H., 2002. Optimum field parameters of an MASW survey [Exp. Abs.]. SEG-J, Tokyo, May, 22-23.

Park, C.B., Miller, R.D., Xia, J., 1999. Multi-channel analysis of surface waves. Geophysics 64 (3), 800–808.

Purnachandra Rao, N., 1999. Single station moment tensor inversion for focal mechanisms of Indian intra-plate earthquakes. Current Science 77, 1184–1189.

RaghuKanth, S.T.G., Iyengar, R.N., 2006. Seismic hazard estimation for Mumbai City. Current Science 91 (11), 1486–1494.

RaghuKanth, S.T.G., Iyengar, R.N., 2007. Estimation of seismic spectral acceleration in peninsular India. Journal of Earth System Science 116 (3), 199–214.

Ramalingeswara Rao, B., 2000. Historical Seismicity and deformation rates in the Indian Peninsular Shield. Journal of Seismology 4, 247–258.

Sitharam, T.G., Anbazhagan, P., Ganesha Raj, K., 2006. Use of remote sensing and seismotectonic parameters for seismic hazard analysis of Bangalore. Natural Hazards Earth System Science 6, 927–939.

Sitharam, T.G., Anbazhagan, P., 2007. Seismic hazard analysis for Bangalore Region. Journal of Natural Hazards 40, 261–278.

Sridevi, Jade, 2004. Estimation of plate velocity and crustal deformation in the Indian subcontinent using GPS geodesy. Current Science 86, 1443–1448.

Stokoe II, K.H., Wright, G.W., James, A.B., Jose, M.R., 1994. Characterization of geotechnical sites by SASW method. In: Woods, R.D. (Ed.), Geophysical Characterization of Sites: ISSMFE Technical Committee #10. Oxford Publishers, New Delhi.

Tokimatsu, K., 1995. Geotechnical site characterization using surface waves. Proc. 1st Int. Conf. on Earth. Geotechn. Eng. IS-Tokyo, p. 36.

Xia, J., Miller, R.D., Park, C.B., 1999. Estimation of near-surface shear-wave velocity by inversion of Rayleigh wave. Geophysics 64 (3), 691–700.

Xu, Y., Xia, J., Miller, R.D., 2006. Quantitative estimation of minimum offset for multichannel surface-wave survey with actively exciting source. Journal of Applied Geophysics 59 (2), 117–125.

Zhang, S.X., Chan, L.S., Xia, J., 2004. The selection of field acquisition parameters for dispersion images from multichannel surface wave data. Pure and Applied Geophysics 161, 185–201.